Pakistan Veterinary Journal

ISSN: 0253-8318 (PRINT), 2074-7764 (ONLINE)
DOI: 10.29261/pakvetj/2024.289

RESEARCH ARTICLE

Effect of *Tupistra chinensis baker* therapy on intestinal injury induced by *Escherichia coli*

Xiaocong Li[1], Chang Xu[2], Jiadong Chen[2], Yao Xie[2], Yaoyan Dun[2], Chengxiong Liu[3], Zhaoxia Liu[3], Dalia Fouad[4], Sammina Mahmood[5], Shuhong Shen[1*] and Kun Li[2*]

[1]Hubei Three Gorges Polytechnic, Yichang 443000, China.
[2]College of Veterinary Medicine, Nanjing Agricultural University, Nanjing 210095, China.
[3]Key Laboratory of Natural Products Research and Utilization in Hubei Province, China Three Gorges University, Yichang 443002, China.
[4]Department of Zoology, College of Science, King Saud University, PO Box 22452, Riyadh 11495, Saudi Arabia.
[5]Department of Botany, Division of Science and Technology, University of Education, Lahore, Pakistan.
*Corresponding author: Kun Li (lik2014@sina.com); Shuhong Shen (478638510@qq.com)

ARTICLE HISTORY (24-603)

Received: October 6, 2024
Revised: November 21, 2024
Accepted: November 22, 2024
Published online: December 6, 2024

Key words:
16S rRNA sequencing
Escherichia coli
Gut microbiota
Tupistra chinensis Baker
Bacterial diarrhea

ABSTRACT

Bacterial diarrhea remains a significant global challenge in livestock farming, leading to serious animal health issues. The effect of *Tupistra chinensis Baker* therapy on intestinal alternations in *Escherichia coli* (*E. coli*)-infected mice was evaluated in this study. Thirty ICR mice were randomly divided into three groups: CK, PK, and MK. The CK and MK groups received normal saline intragastrical for 14 days, while the PK group was administered TCB polysaccharide solution for the same period. On the 14th day, the CK group was given PBS intragastrical while the MK and PK groups received an *E. coli* solution (8×10^9CFU). Serum inflammatory factors and oxidative stress indexes were determined. Total fecal DNA was extracted for amplification, amplified products were processed for sequencing by MiSeq sequencer. The histopathology analysis revealed that the intestinal injury in the PK group was mitigated, with increased villi height and less crypt depth compared to the MK group. The serum levels of inflammatory cytokines IL-1β, IL-6, and IL-10 were significantly restored in the PK group compared to the MK group ($P<0.0001$). Moreover, the antioxidant capacity was enhanced considerably, as indicated by increased SOD and GSH-px levels. Additionally, intestinal microbiota sequencing identified 25 distinct genera, including butyrate-producing bacteria such as *Dysosmobacter* ($P<0.05$), *Angelakisella* ($P<0.05$), *Lachnoclostridium_B* ($P<0.01$), and *Eubacterium_J* ($P<0.01$). Conversely, pathogenic genera such as *Alloprevotella* ($P<0.05$), *Adlercreutzia* ($P<0.05$), and *Muribaculum* ($P<0.05$) were reduced in the PK group. In conclusion, TCB can potentially protect the gut from oxidative stress and inflammation caused by *E. coli* infection.

To Cite This Article: Li X, Xu C, Chen J, Xie Y, Dun Y, Liu C, Liu Z, Fouad D, Mahmood S, Shen S and Li K, 2024. Effect of *Tupistra chinensis baker* therapy on intestinal injury induced by *Escherichia coli*. Pak Vet J, 44(4): 1033-1042. http://dx.doi.org/10.29261/pakvetj/2024.289

INTRODUCTION

Diarrhea caused by various diseases poses a significant challenge to animal health (Khan *et al.,* 2022; Li *et al.,* 2023), while in calves, diarrhea leads to higher mortality rates and greater economic losses compared to other livestock (Jacobson, 2022; Wong *et al.,* 2022). Calf diarrhea is a leading cause of poor growth and development in young cattle, significantly affecting overall health and productivity (Anwar *et al.,* 2022; Zhang *et al.,* 2024). The etiological factors of calf diarrhea include bacterial infections (Jacobson, 2022), viral pathogens (Hodnik *et al.,* 2020), parasitic infestations (Geng *et al.,* 2021), and non-infectious causes such as nutritional deficiencies. Bacterial infections are a common cause of calf diarrhea. The primary mechanism of diarrhea is bacterial overgrowth in the intestine, which disrupts the balance of intestinal flora and severely damages the intestinal mucosal barrier (Saffouri *et al.,* 2019). *Escherichia coli* (*E. coli*) is the most prevalent bacterial pathogen responsible for calf diarrhea, contributing to intestinal infections (Mohammed *et al.,* 2019; Rasheed *et al.,* 2023). Under a conducive environment, *E. coli* can cause gastrointestinal infections,

while in severe cases, it spreads to other tissues and organs leading to systemic complications (Lee *et al.*, 2022). *E. coli* infection leads to a substantial increase in bacterial load in the intestine, disrupting the microbial balance and resulting in diarrhea (Moran-Garcia *et al.*, 2022). Currently, antibiotics are the primary therapy for *E. coli*-induced diarrhea. However, the increasing prevalence of antibiotic-resistant bacteria and widespread antibiotic misuse (Jia *et al.*, 2022), have prompted research into safe and reliable alternatives for managing calf diarrhea.

Intestinal beneficial flora consists of bacteria, fungi, and other microorganisms that inhabit the guts, forming a biological barrier to protect and maintain the integrity of the intestinal mucosa (Glassner *et al.* 2020). The gut microbiota plays a crucial role in nutrient absorption (Li *et al.*, 2024a), immune defense (Zhou *et al.*, 2020), regulation of metabolism, and other essential physiological functions. One of the primary nutritional functions of gut bacteria is the production of short-chain fatty acids (SCFAs) through the fermentation of dietary fibers. SCFAs such as butyrate, lower the pH in the colon, inhibiting the growth of harmful bacteria, and supporting intestinal health by preventing dysfunction (Martin-Gallausiaux *et al.*, 2021). There is a strong link between the gut flora and the immune system. Gut flora plays an important role in developing immune defense by regulating both innate and adaptive immune responses as well as maintaining a balance between inflammatory and anti-inflammatory activities (Wiertsema *et al.*, 2021). Gut microbiota also influences the host's lipid metabolism by production of metabolites like SCFAs, Polyunsaturated fatty acids, secondary bile acids, and trimethylamine. Moreover, pro-inflammatory bacterial components such as lipopolysaccharides contribute to metabolic regulation (Schoeler and Caesar, 2019; Brown *et al.*, 2023). Gut microbiota has been shown to regulate glucose metabolism and is also involved in the metabolism of bile acid (Cai *et al.*, 2022).

Traditional Chinese medicine plays a unique role in the treatment of various diseases due to its synergistic regulation of multiple components, targets, and pathways (Zhao *et al.*, 2023). *Tupistra chinensis Baker* (TCB) is a well-known traditional Chinese medicinal herb with a long history of therapeutic use. It is characterized by bitter taste and cold properties. TCB has been traditionally indicated for treating ailments of throat swelling, diphtheria, cancer, stomach pain, and snake bites (Wang *et al.*, 2021; Lu *et al.*, 2023). Modern pharmacological studies have demonstrated significant antibacterial (An *et al.*, 2020), anti-inflammatory (Xu *et al.*, 2020), anti-tumor, antioxidant (Wang *et al.*, 2020a; Wang *et al.*, 2021) and immune-regulating effects of TCB. The main active components of TCB include steroids (spirosteroids, furosteroids), saponins, polysaccharides, and flavonoids. The current studies on TCB have mainly focused on its saponin content, while studies investigating its polysaccharides remain limited (Xu *et al.*, 2020; He *et al.*, 2023). Therefore, this study evaluates the therapeutic effect of TCB polysaccharides on bacterial diarrhea by examining their influence on inflammation, oxidative stress, and gut microbiota. This study aims to explore novel approaches for treating diarrhea from a new perspective.

MATERIALS AND METHODS

Drugs and reagents: *Tupistra chinensis Baker* roots were chopped and finely ground. The ground roots were soaked in triploid 95% ethanol and subjected to Soxhlet extraction to remove fat until the ether extract turned colorless at 45℃. The resulting residues were dried and refluxed with 95% ethanol for 2 hours at 90℃. This process was repeated twice to eliminate monosaccharides, oligosaccharides, and other alcohol-soluble impurities. After drying, the residue was extracted by refluxing with distilled water at 90℃ in water baths three times for 2 hours each. The filtrates were combined and concentrated to an appropriate volume under reduced pressure. An equal volume of 95% ethanol was added to the concentrated filtrate and the mixture was left to stand overnight. The resulting precipitate was collected by vacuum filtration to obtain solid material. The solid material was washed three times with anhydrous ethanol, acetone, and ether, then dried at 50℃ to obtain crude polysaccharide.

Animals and experiment design: The approval was granted by the Experimental Animal Ethics Center of Nanjing Agricultural University. Thirty male and female ICR mice were provided by Yangzhou University. The mice underwent a 3-day adaptation period and a 12-hour light-dark cycle in the laboratory. The mice were randomly divided into three groups (n=10, with an equal distribution of male and female mice); CK group, MK group, and PK group. The polysaccharide treatment group received 1g/kg polysaccharide solution daily, while the control and model groups were administered 0.5mL of normal saline daily via oral gavage for 14 consecutive days. One hour after the last administration, mice in the model and polysaccharide group were administered with *E. coli* 8×10^9CFU (0.2mL PBS) (Ren *et al.*, 2022), while the CK group was administered with 0.2mL PBS through gavage. The *Escherichia coli* used was isolated from the feces of diarrheal yaks. After 24 hours of administration, mice were euthanized to collect blood samples from the orbital venous plexus of mice to obtain serum. Afterward, intestinal tissue samples were collected for subsequent histopathology and molecular analysis (Fig. 1).

Serum inflammatory factors and oxidative stress indexes: Blood collected from the mice were transferred into 1.5mL centrifuge tubes and centrifuged at 3500rpm for 15 minutes at 4°C to obtain serum. The serum levels of MDA, SOD, GSH-px, and total antioxidant capacity (T-AOC) were determined using commercial kits provided by Jianglai Biotechnology Co., Ltd, China. Inflammatory cytokines including IL-10, IL-6, IL-1β, and TNF-α were measured using ELISA kits (Nanjing Jiancheng Bioengineering Institute, China).

Histopathological analysis of the intestine: Intestinal samples were fixed in 4% paraformaldehyde for at least 48 hours for subsequent H&E staining (Pinuofei Biological Technology, Wudwa-China). The intestinal morphology was examined using an Olympus CX23 microscope (Olympus Co., Japan).

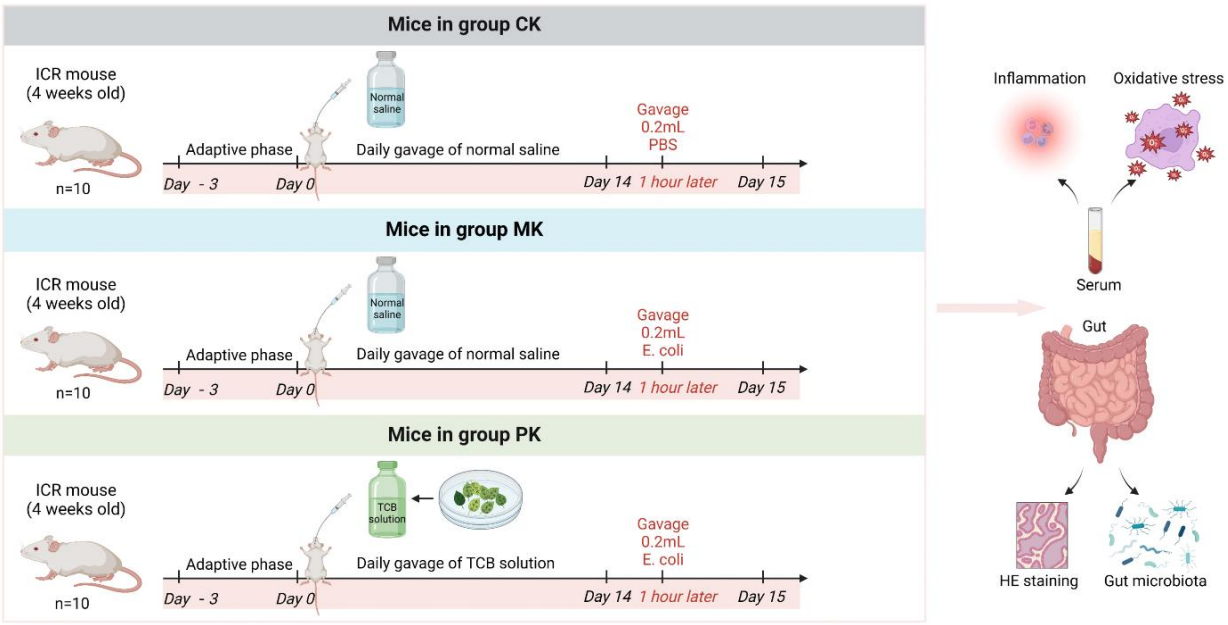

Fig. 1: Flow chart of animal experiment.

Table 1: The sequenced data of mice microbiome

Sample ID	Input	Filtered	Denoised	Merged	Non-chimeric	Non-singleton
CK1	74002	68543	66620	56451	43534	43359
CK2	74107	68146	66794	60221	45095	44989
CK3	83376	77342	74728	61434	41897	41517
CK4	84438	78332	75815	59440	41501	41238
CK5	86378	80434	77930	64261	50405	50183
CK6	76367	70778	67822	52915	40155	39878
MK1	75964	70488	68808	59718	42839	42600
MK2	63547	58810	57653	50881	39422	39152
MK3	71019	65962	64179	55495	38031	37741
MK4	74767	68999	66624	52510	40200	39924
MK5	70134	64626	63082	55143	45509	45351
MK6	73465	68176	66309	53726	42345	42127
PK1	61747	57421	56567	52382	42275	42117
PK2	66919	62219	60700	50908	31917	31449
PK3	71283	65819	64305	55374	39183	38924
PK4	68328	63253	61976	54329	40294	40109
PK5	76218	70516	69051	60116	41245	41023
PK6	74204	68791	67295	58153	40548	40239

Total fecal DNA extraction and 16S rRNA high-throughput sequencing: Total fecal DNA was extracted from commercial kits. DNA concentration was quantified by Nanodrop spectrophotometer, and quality was detected by 1.5% agarose gel electrophoresis (Yo *et al.*, 2024). The V3-V4 variable region of the bacterial 16S rRNA gene was amplified using the universal primers 338F: 5 '-ACTCCTACGGGAGGCAGCA-3' and 806R:5 '-GGACTACHVGGGTWTCTAAT-3' (Guivala *et al.*, 2024).

PCR amplification was performed using Pfu high-fidelity DNA polymerase (Quanshi Gold Company). Amplification products were purified for sequencing. Paired-end sequencing was performed by MiSeq sequencer.

Bioinformatics analysis of sequencing results: Raw sequencing data were processed using the QIIME2 DADA2 method, which included primer removal, quality filtering, and generating high-quality feature sequences (Balzerani *et al.*, 2024). The abundance table was flattened to ensure even sampling depth, and rarefaction and species accumulation curves were generated to evaluate sequencing depth and data volume. Then, α diversity analysis was performed to describe microbial diversity within each group. Moreover, β-diversity analysis was performed to assess differences in microbial community composition between groups. Differential flora metabolic pathways were identified using LEfSe.

RESULTS

Impact of *Tupistra chinensis Baker* on intestinal damage caused by *E. coli:* In this study, H&E staining of the jejunum was utilized to assess the intestinal injury and the therapeutic effects of TCB in mice. In the CK group, the intestinal epithelial cells exhibited uniform morphology, and the villi were well-organized and intact (Fig. 2a). In the *E. coli* challenge group, a significant thinning of the intestinal wall was observed, accompanied by infiltration of inflammatory cells. There was marked atrophy, deformation, and rupture of intestinal villi, resulting in shortened villi, and increased crypt depth (Fig. 2b). In the PK group, partial restoration of villi length, with shallower crypt depth, and more organized villus arrangement was seen, resembling the control group (Fig. 2b).

***Tupistra chinensis Baker* alleviates inflammation and oxidative stress in mice:** Compared to the control group, serum levels of inflammatory cytokines IL-1β, IL-6, IL-10, and TNF-α in the PK group were significantly increased ($P<0.0001$) (Fig. 3). However, after TCB treatment, the cytokines levels in the PK group were notably reduced, approaching those of the control group. In addition, oxidative stress indicators were also affected by *E. coli* infection. MDA level increased, while TAOC, SOD ($P<0.05$) and GSH-px ($P<0.05$) significantly decreased. Interestingly, TCB treatment significantly reversed the changes in serum markers caused by *E. coli* infection. The levels of inflammatory cytokines and oxidative stress markers in the PK group were nearly restored to the control group level, indicating the improvement in both inflammatory response and antioxidant capacity.

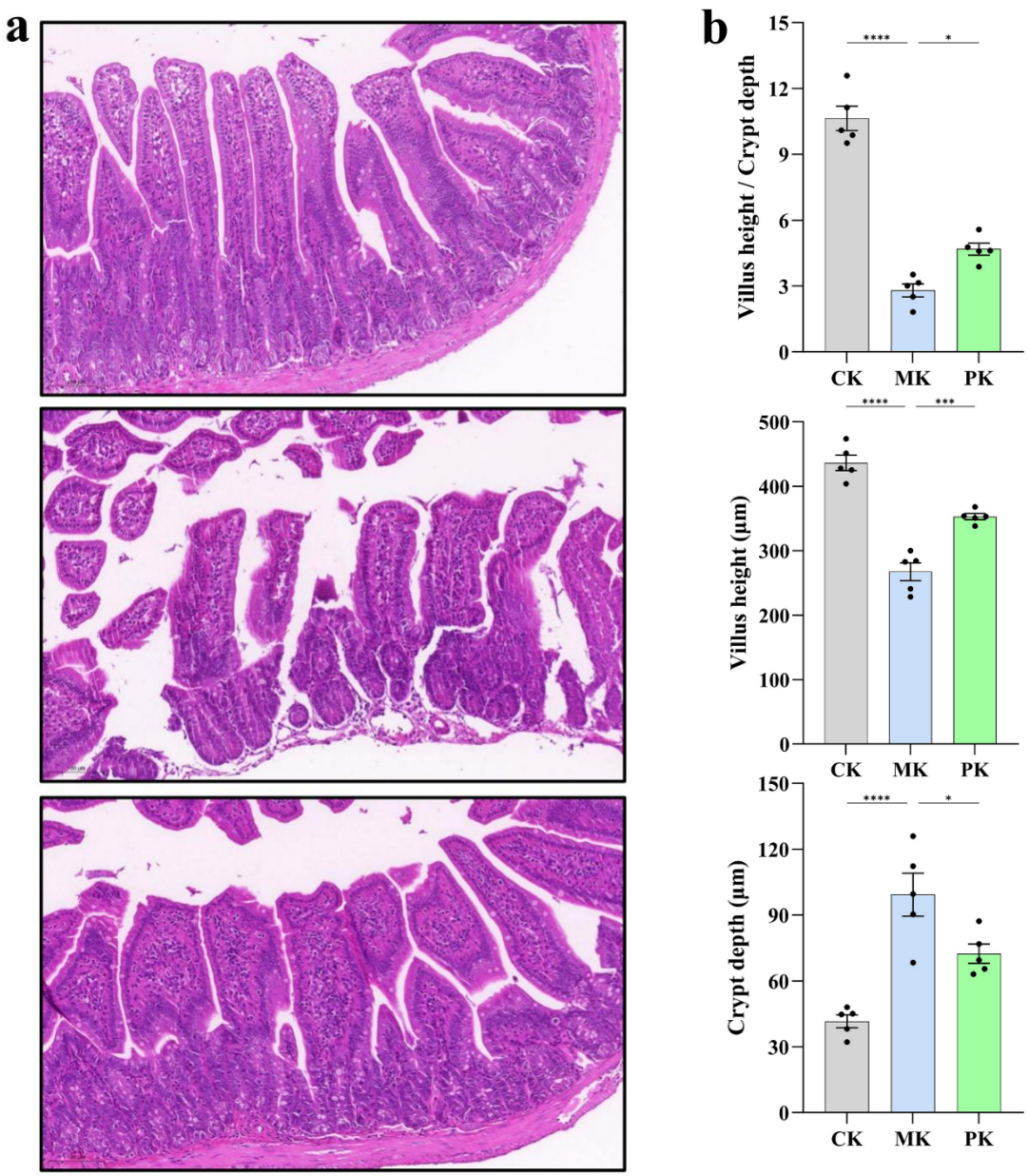

Fig. 2: Intestinal pathological changes in CK, MK, and PK groups. *P<0.05; ***P<0.001; ****P<0.0001.

Sequencing data results of TCB treatment for *E. coli* diarrhea: A total of 18 rectal contents (n=6 in each group) were selected for amplicon sequencing. The CK, MK, and PK groups yielded 74,000, 63,000, and 61,000 raw data reads, respectively. After that, each sample retained between 57653 and 77930 reads, resulting in a total of 1196258 clean reads from all 18 samples (Table 1). In addition, the Venn map showed 16,192 ASVs across the three groups, with 482 ASVs shared among all groups. The CK and MK groups shared 888 ASVs, the PK group had 745 unique ASVs (Fig. 4a).

Effect of *Tupistra chinensis Baker* treatment on gut microbiome structure: We performed Chao1, Faith_pd, Goods_coverage, observed_species, Pielou's evenness, and other α diversity analyses on the intestinal microorganisms of the three groups of mice. No significant differences were observed among the groups, indicating minimal variation between the samples in each experimental group (Fig. 4b). The rarefaction curve and rank-abundance curve gradually leveled off, suggesting sequencing depth sufficient to reflect the microbial diversity in the samples (Fig. 4c-d).

At the phylum level, Firmicutes_D, Firmicutes_A and Bacteroidota were the most abundant bacteria in CK (31.47, 32.67, and 28.80%), MK (43.71, 16.45, and 34.49%) and PK (41.87, 6.65 and 46.85%) groups, respectively (Fig. 5a). At the class level, we observed microflora differences among the experimental groups. Clostridia_258483 was the dominant class in the CK group (32.68%) but was less abundant in the MK (16.46%) and PK group (6.65%). Bacilli (43.71%) dominated the MK group, while Bacteroidia (46.85%) was the most abundant in the PK group. Bacilli (31.47%) and Bacteroidia (28.81%) also showed high abundances in the control group. In the MK group, Bacteroidia (34.49%) and Clostridia_258483 (16.46%) were among the top three classes. Similarly, Bacilli (41.87%) and Clostridia_258483 (6.65%) constituted a large proportion of the PK group (Fig. 5b). At the order level, the primary orders shared by CK, MK, and PK

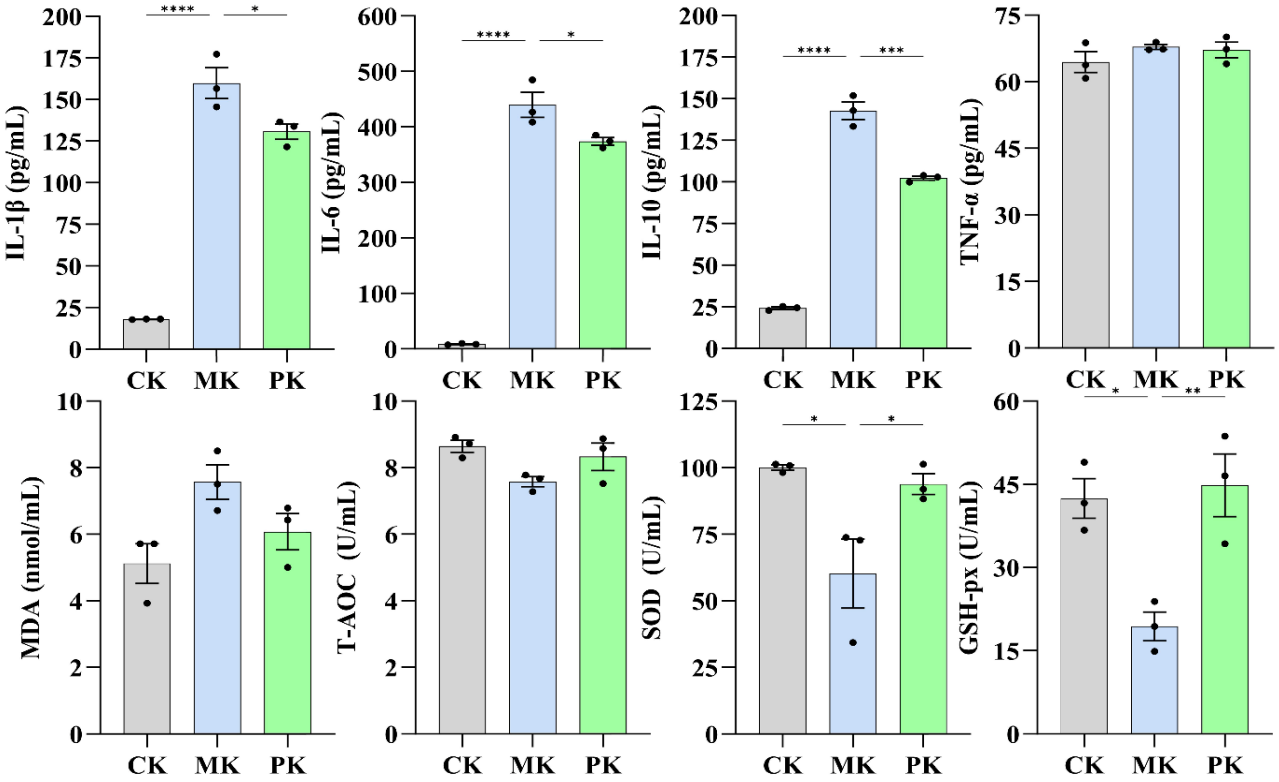

Fig. 3: Effects of *Tupistra chinensis Baker* on serum inflammatory factors and antioxidant capacity in mice. *P<0.05; **P<0.01; ***P<0.001; ****P<0.0001.

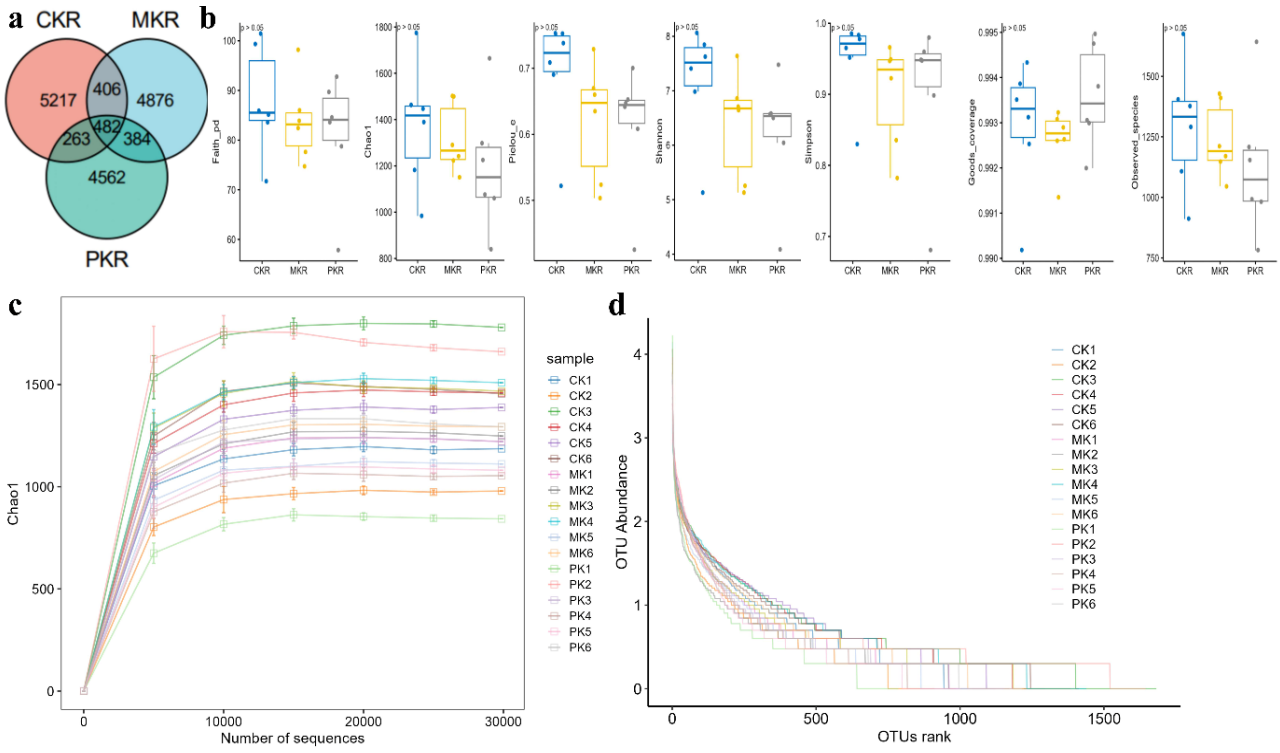

Fig. 4: Alpha diversity analysis of microbiome in different groups. a: Venn map, b: indexes, c: rarefaction curve, d: rank abundance curve.

groups were Lactobacilli (30.53, 43.15, and 41.23%), Bacteroidetes (27.61, 34.14, and 46.45%), and Spirochaeta (23.13, 11.50, and 3.73%) (Fig. 5c). At the family level, the predominant families in the CK and MK groups were Lactobacillaceae (30.37 and 41.18%), Lachnospiraceae (23.09 and 11.48%) and Muribaculaceae (18.85 and 25.88%). Meanwhile, the PK group was primarily composed of Lactobacillaceae (39.17%), Muribaculaceae (34.40%) and Bacteroidaceae (7.70%) (Fig. 5d). At the genus level, *Lactobacillus* (20.43, 25.62 and 27.97%) was the dominant genus common to all three groups (CK, MK and PK). Furthermore, the CK group contained substantial

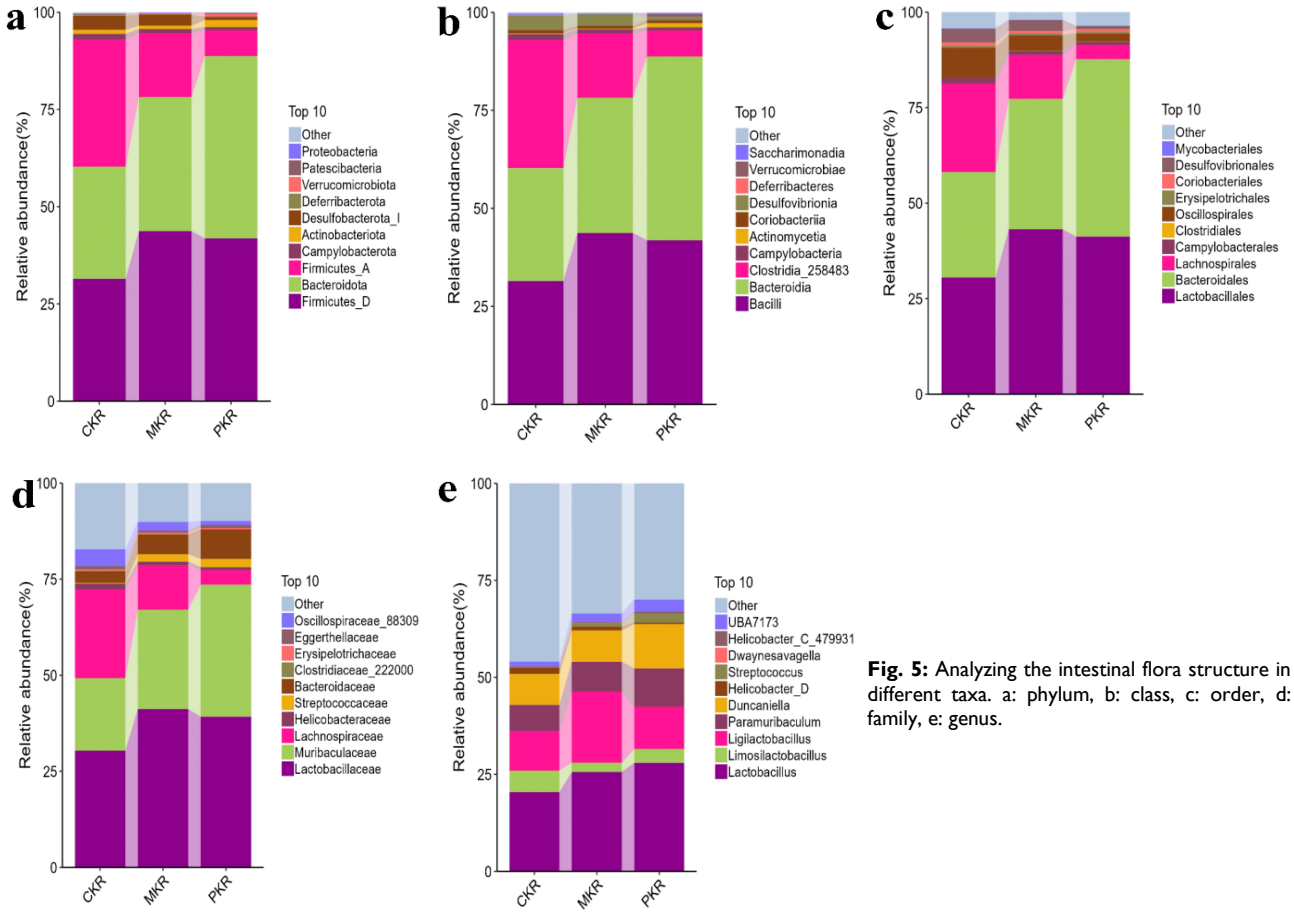

Fig. 5: Analyzing the intestinal flora structure in different taxa. a: phylum, b: class, c: order, d: family, e: genus.

proportions of *Ligilactobacillus* (10.27%), *Duncaniella* (7.99%), *Paramuribaculum* (6.67%), *Limosilactobacillus* (5.54%), *Mailhella* (3.61%) and *Rikenella* (2.46%). The MK group was dominated by *Ligilactobacillus* (18.34%), *Duncaniella* (8.06%), *Paramuribaculum* (7.69%), and *Alloprevotella* (3.20%). Interestingly, *Duncaniella* (11.47%) was the second most abundant genus in the CK group, while *Ligilactobacillus* (10.89%), *Paramuribaculum* (9.84%), *Alloprevotella* (4.25%), *Limosilactobacillus* (3.57%) and *Bacteroides_H* (3.47%) were also prevalent in the CK group (Fig. 5e).

Tupistra chinensis Baker* treatment affected the marker species in mice challenged with *E. coli: PCoA and NMDS analysis showed no significant difference between the three groups (Fig. 6a and 6b). Interestingly, LDA scores and phylogenetic cladistics at the genus level indicated partial differences in microbial flora (Fig. 6c). We identified a total of 23 distinct genera. Compared to the CK group, the *E. coli* challenge significantly increased the abundance of *Alloprevotella* (P<0.05), *UBA7173* (P<0.05), *UBA3263* (P<0.05), *Muribaculum* (P<0.05), *Eubacterium_R* (P<0.05) and *Soleaferrea* (P<0.05). Interestingly, the genera were significantly reduced in the PK group, approaching the level seen in the normal control group. Meanwhile, in the MK group, there was a significant decrease in the abundance of *UBA3282* (P<0.01), *Adlercreutzia_404257* (P<0.05), *Desulfovibrio_R_446353* (P<0.05), *Lawsonibacter* (P<0.01), *UBA9715* (P<0.05), *Eubacterium_J* (P<0.01), *14-2* (P<0.05), *Dysosmobacter* (P<0.05), *Borkfalkia* (P<0.05), *Angelakisella* (P<0.05), *Acutalibacter* (P<0.05), *Merdibacter* (P<0.05), *Coprocola* (P<0.05), *Massilioclostridium* (P<0.01), *Lachnoclostridium_B* (P<0.01), *Emergencia* (P<0.05), *Cupidesulfovibrio* (P<0.05), *Staphylococcus* (P<0.05) and *Enterococcus_B* (P<0.0001) compared with the CK group. In the TCB treatment group except for Adlercreutzia_404257 and Merdibacter, the abundance of other bacteria was higher than in the MK group and even exceeded in the CK group (Fig. 7).

***Tupistra chinensis Baker* affected microbial metabolic pathways:** We utilized MetaCyc and KEGG databases to analyze LDA scores related to metabolic pathways. As depicted in Fig. 8, the MetaCyc database revealed that PWY-5505, PWY-5509, PWY-6269, ARGSYN-PWY, PWY-7400, PWY-6588, PWY-5676, PWY-6353, PWY-6608, and SALVADEHYPOX-PWY pathways exhibited significantly higher LDA scores compared to the other two groups. The biotin biosynthesis I pathway in group PK demonstrates a significant decrease (Fig. 8a).

KEGG database analysis revealed that the two-component system and D-Ariginine and D-Omithine metabolism pathway in group CK showed significantly higher scores than the other two groups. Starch and sucrose metabolism was elevated in group MK, while Glycosaminoglycan degradation, amino sugar, and nucleotide sugar metabolism increased in the PK group. Additionally, pathways related to streptomycin biosynthesis, Zeatin biosynthesis, Sphingolipid metabolism, RNA degradation, Nicotinate as well as nicotinamide metabolism, and Oxidative phosphorylation showed significant increases after TCB treatment (Fig. 8b).

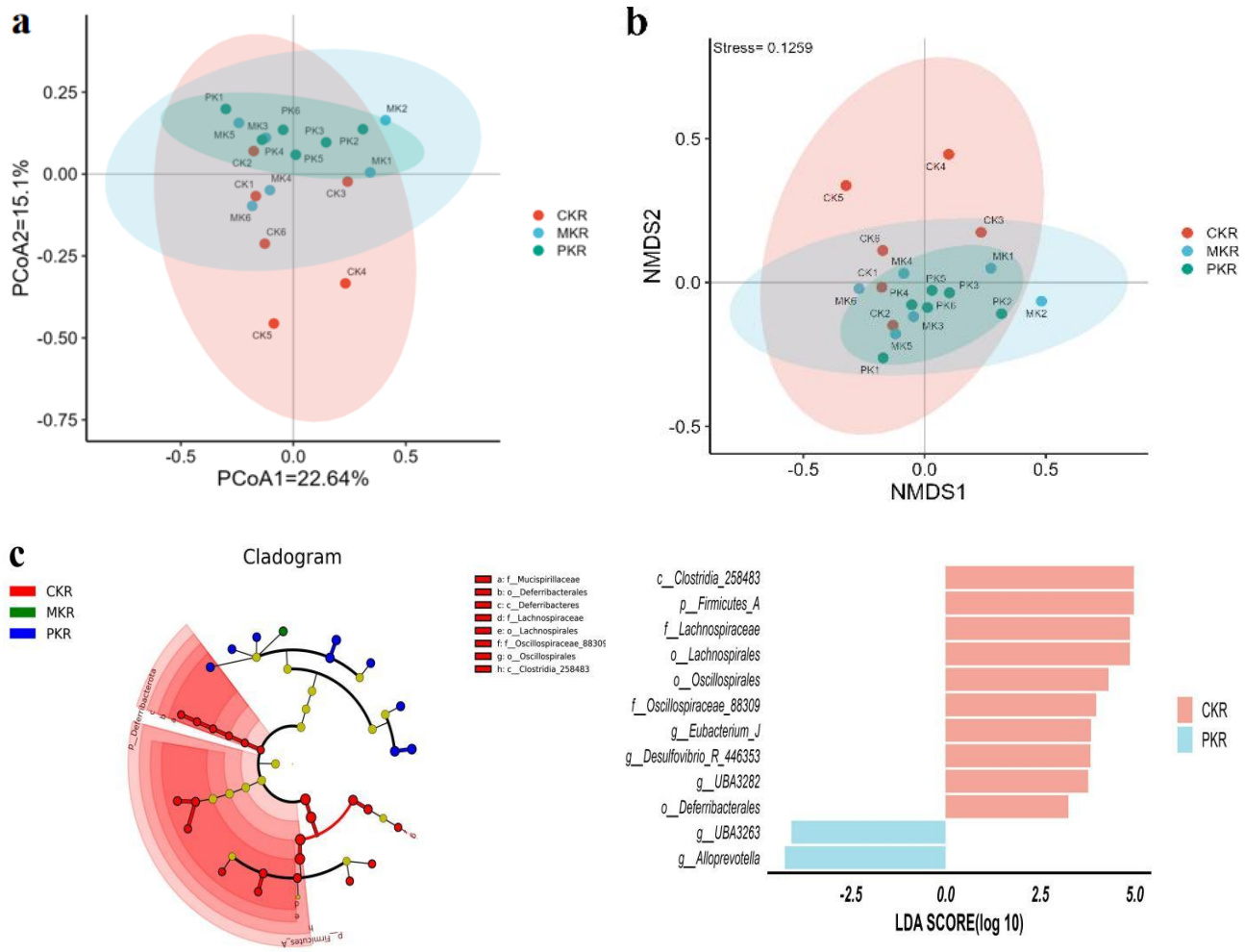

Fig. 6: Beta diversity analysis and the markedly different species between different groups via LEfSe. a: PCoA, b: NMDS, c: LEfSe analysis.

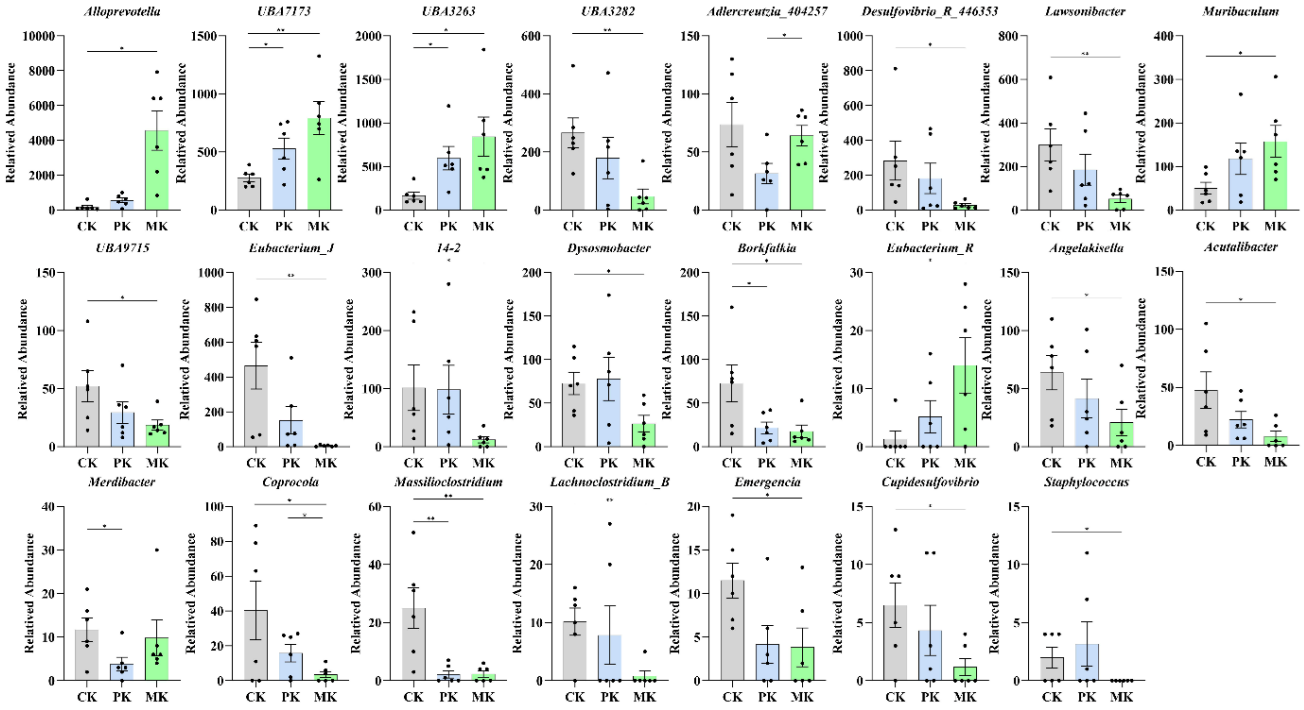

Fig. 7: Differences in the microflora of different groups at gene level. *P<0.05; **P<0.01.

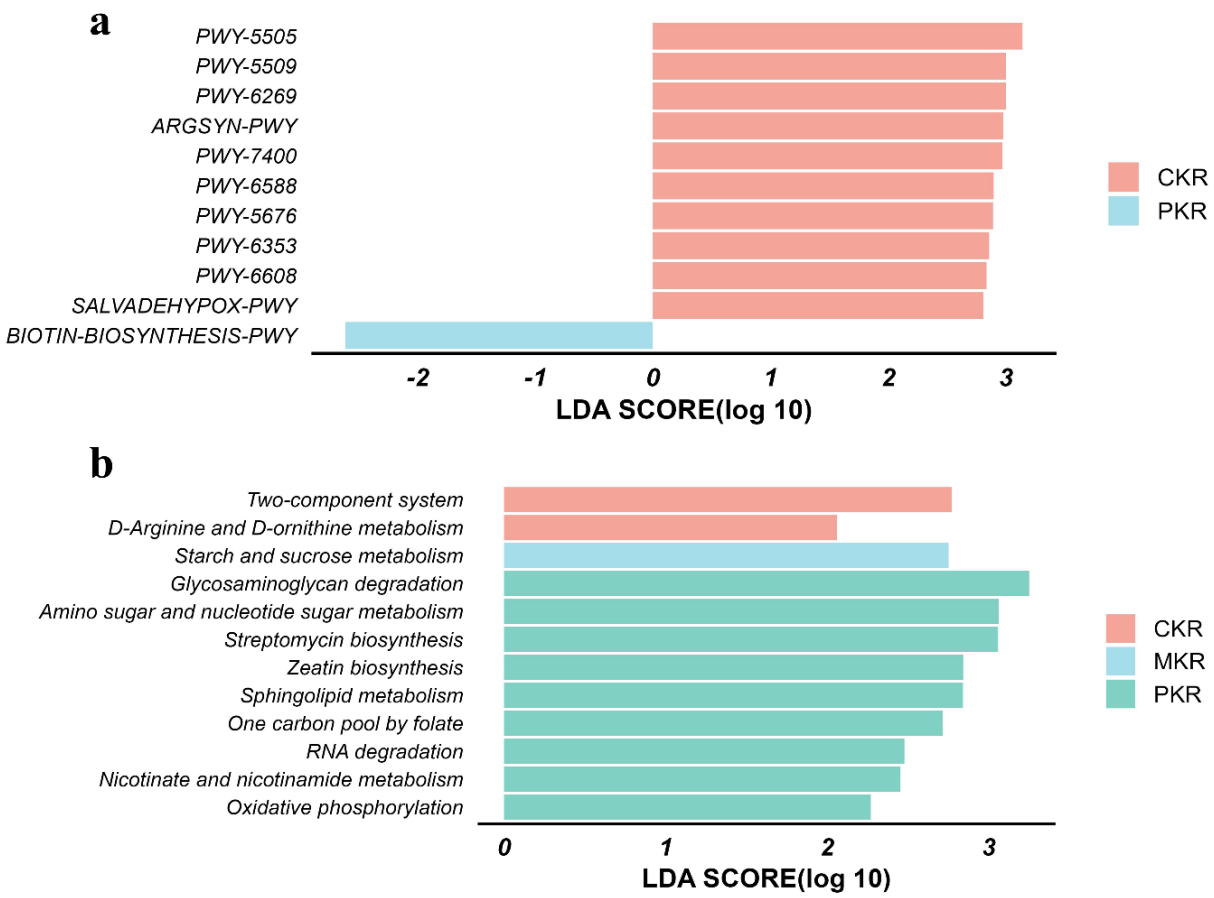

Fig. 8: Analyzing the microbiota function between different groups. a: MetaCyc pathways, b: KEGG pathways.

DISCUSSION

Our study investigated the alleviating effect of *Tupistra chinensis Baker* on gastrointestinal dysfunction caused by *E. coli* infection in mice. Currently, over 200 types of cytokines have been identified to date (Rahman *et al.*, 2023). IL-6 is a multifunctional cytokine, and infection often leads to elevated serum IL-6 levels, which often precede increases in other cytokines (Kang *et al.*, 2020). Inflammation onset is frequently accompanied by substantial secretion of IL-1β, which plays a pivotal role in initiating inflammation in certain diseases e.g. acute gout attacks and the onset of rheumatoid arthritis (Wang *et al.*, 2020b). Interleukin-10 acts as an anti-inflammatory cytokine and recent studies have demonstrated its dual role in immunostimulation and immunosuppression (Saraivan *et al.* 2020). Following TCB treatment, the levels of these three inflammation-related cytokines decreased significantly, indicating that TCB may have the potential to alleviate *E. coli-induced* inflammation. GSH-px and SOD are key indicators for assessing the *in vivo* antioxidant capacity (Yu *et al.*, 2024a). The decrease in the MK group and the increase in the PK group suggest that TCB significantly enhances the antioxidant capacity in animals. These alterations in inflammation and oxidative stress markers are consistent with findings from previous experiments on *Anethum gravelons* fruit extract (AGFAE) in a rat model of castor oil-induced diarrhea (Brinsi *et al.*, 2024).

The gut microbiota is intricately linked to human health, and previous research has demonstrated that diarrhea can disrupt the balance of gut microbiota (Li *et al.*, 2024b). Treatment with TCB restored the perturbed gut microbiome environment. Through correlation analysis, we identified 23 differentially abundant genera. Alloprevotella is considered a biomarker for bile reflux disease and related gastrointestinal disorders (Yang *et al.*, 2022; Zhou *et al.*, 2022). While Adlercreutzia is generally considered a probiotic, it has also been reported to be associated with insulin resistance (Livantsova *et al.*, 2024). Muribaculum has been reported to increase in abundance in diabetic rats with depressive symptoms (Shen *et al.*, 2024). Desulfovibrio_R_446353 is thought to be involved in Lactobacillus-mediated reduction of alcoholic fatty liver in mice (Gu *et al.*, 2024). Lawsonibacter is a butyrate-producing bacterium (Le Sayec *et al.*, 2022), closely related to overall health, and plays a key role in regulating intestinal health, preventing inflammation, and mitigating cancer risk (Huang *et al.*, 2024). Eubacterium_J is a prevalent probiotic that generates butyrate and has been used to treat colitis in mice (Ryu *et al.*, 2024; Visuthranukul *et al.*, 2024). Notably, Dysosmobacter, Angelakisella, and Lachnoclostridium_B are also butyrate producers (Gonzalez *et al.*, 2024; Yi *et al.*, 2024). Butyric acid serves as the preferred energy source for intestinal epithelial cells. Its sodium salt can stimulate the absorption of sodium ions and water in the colon, promote intestinal villus proliferation, facilitate intestinal development, and enhance absorption and utilization (Yu *et al.*, 2024b). The increase in the abundance of butyrate-producing bacteria in the PK treatment group indicates that TCB may restore intestinal damage by regulating the population of butyrate-producing bacteria. In conclusion, TCB treatment enhances

the abundance of beneficial bacteria, restoring the gut microbiota disturbed by *E. coli* infection.

Conclusions: These findings indicated that TCB effectively mitigated intestinal damage in mice, decreased inflammatory markers, and enhanced the antioxidant capacity of the mice. Furthermore, TCB increased the abundance of beneficial intestinal flora and promoted the production of associated metabolites. In conclusion, TCB is a novel therapeutic approach to control bacterial diarrhea.

Data availability: Sequencing data used in this study were stored in the NCBI database under accession number: PRJNA1159924.

Authors contribution: XCL, KL, and SHS: research idea and methodology. XCL, CX, JDC, YX, YYD, CXL, and ZXL: reagents, materials, analysis tools, and writing – review and editing. KL, DF, and SHS: writing – original draft preparation, review, and editing. KL and JMJ: visualization and supervision. All authors know and approve the final manuscript.

Acknowledgments: This work was supported by the Science and Technology Innovation Funds of Yichang city (A24-3-032) and the Doctoral Special Fund of Hubei Three Gorges Polytechnic (2024ZX02). The authors extend their appreciation to Researchers Supporting Project number (RSPD2025R965), King Saud University, Riyadh, Saudi Arabia.

REFERENCES

An C, Ma S, Shi X, *et al*., 2020. Isolation, diversity, and antimicrobial activity of fungal endophytes from Rohdea chinensis (Baker) N. Tanaka (synonym Tupistra chinensis Baker) of Qinling Mountains, China. Peer J 8:e9342.

Anwar MA, Aziz S, Ashfaq K, *et al.,* 2022. Trends in frequency, potential risks, and antibiogram of *E. coli* isolated from semi-intensive dairy systems. Pak Vet J 42(2): 167-172.

Balzerani F, Blasco T, Pérez-Burillo S, *et al*., 2024. q2-metnet: QIIME2 package to analyze 16S rRNA data via high-quality metabolic reconstructions of the human gut microbiota. Bioinforma Oxf Engl 40(11):btae455.

Brinsi C, Jedidi S, Sammari H, *et al*., 2024. Antidiarrheal, anti-inflammatory and antioxidant effects of Anethum graveolens L. fruit extract on castor oil-induced diarrhea in rats. Neurogastroenterol Motil 36(11):e14892.

Brown EM, Clardy J and Xavier RJ, 2023. Gut microbiome lipid metabolism and its impact on host physiology. Cell Host Microbe 31:173–186.

Cai J, Sun L and Gonzalez FJ, 2022. Gut microbiota-derived bile acids in intestinal immunity, inflammation, and tumorigenesis. Cell Host Microbe 30:289–300.

Geng H-L, Ni H-B, Li J-H, *et al*., 2021. Prevalence of Cryptosporidium spp. in Yaks (Bos grunniens) in China: A Systematic Review and Meta-Analysis. Front Cell Infect Microbiol 11:770612.

Glassner KL, Abraham BP and Quigley EMM, 2020. The microbiome and inflammatory bowel disease. J Allergy Clin Immunol 145:16–27.

Gonzalez E, Lee MD, Tierney BT, *et al*., 2024. Spaceflight alters host-gut microbiota interactions. NPJ Biofilms Microbiomes 10:71.

Gu J, Chen Y, Wang J, *et al*., 2024. *Lacticaseibacillus rhamnosus* LRa05 alleviated liver injury in mice with alcoholic fatty liver disease by improving intestinal permeability and balancing gut microbiota. Benef Microbes 15:481–493.

Guivala SJ, Bode KA, Okun JG, *et al*., 2024. Interactions between the gut microbiome, associated metabolites and the manifestation and progression of heart failure with preserved ejection fraction in ZSF1 rats. Cardiovasc Diabetol 23:299.

He X, Yuan X, Liu Y, *et al*., 2023. Three New Steriodal Saponins from the Rhizomes of Tupistra chinensis Baker. Chem Biodivers 20: e202201129.

Hodnik JJ, Ježek J and Starič J, 2020. Coronaviruses in cattle. Trop Anim Health Prod 52:2809–2816.

Huang B, Yin T, Fu S, *et al*., 2024. Inflammation-oriented montmorillonite adjuvant enhanced oral delivery of anti-TNF-α nanobody against inflammatory bowel disease. Proc Natl Acad Sci U S A 121:e2320482121.

Jacobson M, 2022. On the infectious causes of neonatal piglet diarrhoea-A Review. Vet Sci 9(8):422.

Jia Y, Mao W, Liu B, *et al*., 2022. Study on the drug resistance and pathogenicity of *Escherichia coli* isolated from calf diarrhea and the distribution of virulence genes and antimicrobial resistance genes. Front Microbiol 13:992111.

Kang S, Narazaki M, Metwally H, *et al*., 2020. Historical overview of the interleukin-6 family cytokine. J Exp Med 217(5):e20190347.

Khan AY, Ahmad SS, Avais M *et al.,* 2022. Molecular prevalence with associated risk factors and haemato-serum electrolyte analysis of *E. coli* O157:H7 in Canine pups with diarrhoea. Pak Vet J 42(2): 161-166.

Le Sayec M, Xu Y, Laiola M, *et al*., 2022. The effects of Aronia berry (poly)phenol supplementation on arterial function and the gut microbiome in middle aged men and women: Results from a randomized controlled trial. Clin Nutr Edinb Scotl 41:2549–2561.

Lee JB, Kim SK and Yoon JW, 2022. Pathophysiology of enteropathogenic *Escherichia coli* during a host infection. J Vet Sci 23:e28.

Li T-T, Chen X, Huo D, *et al.,* 2024a. Microbiota metabolism of intestinal amino acids impacts host nutrient homeostasis and physiology. Cell Host Microbe 32:661-675.e10.

Li X, Zhu X and Xue Y, 2023. Drug resistance and genetic relatedness of *Escherichia coli* from mink in Northeast China. Pak Vet J 43(4): 824-827.

Li Y, Chen Y, Liao Z, *et al*., 2024b. WenTongGanPi decoction alleviates diarrhea-predominant irritable bowel syndrome by improving intestinal barrier. J Ethnopharmacol 334:118544.

Livantsova EN, Leonov GE, Starodubova AV, *et al*., 2024. Diet and the gut microbiome as determinants modulating metabolic outcomes in young obese adults. Biomedicines 12(7):1601.

Lu Y, He X, Liu Y, *et al*., 2023. Steriodal saponins from the rhizomes of *Tupistra chinensis* Baker. Phytochemistry 207:113583.

Martin-Gallausiaux C, Marinelli L, Blottière HM, *et al*., 2021. SCFA: mechanisms and functional importance in the gut. Proc Nutr Soc 80:37–49.

Mohammed SAE-M, Marouf SAE-M, Erfana AM, *et al*., 2019. Risk factors associated with *E. coli* causing neonatal calf diarrhea. Saudi J Biol Sci 26:1084–1088.

Moran-Garcia N, Lopez-Saucedo C, Becerra A, *et al*., 2022. A novel adult murine model of typical enteroaggregative *Escherichia coli* infection reveals microbiota dysbiosis, mucus secretion, and AAF/II-mediated expression and localization of β-catenin and expression of MUC1 in ileum. Front Cell Infect Microbiol 12:885191.

Rahman T, Das A, Abir MH, *et al*., 2023. Cytokines and their role as immunotherapeutics and vaccine Adjuvants: The emerging concepts. Cytokine 169:156268.

Rasheed MB, Ahsan A, Irshad H, *et al.,* 2023. Occurrence of shiga toxin-producing *E. coli* in zoo animals of Rawalpindi and Islamabad zoos. Asian J Agric Biol 2023(2):2022080.

Ren S, Wang C, Chen A, *et al*., 2022. The probiotic *Lactobacillus paracasei* ameliorates diarrhea caused by *Escherichia coli* O(8) via gut microbiota modulation. Front Nutr 9:878808.

Ryu H-M, Islam SMS, Riaz B, *et al*., 2024. Immunomodulatory effects of a probiotic mixture: alleviating colitis in a mouse model through modulation of cell activation markers and the gut microbiota. Int J Mol Sci 25(16):8571.

Saffouri GB, Shields-Cutler RR, Chen J, *et al*., 2019. Small intestinal microbial dysbiosis underlies symptoms associated with functional gastrointestinal disorders. Nat Commun 10:2012.

Saraiva M, Vieira P and O'Garra A, 2020. Biology and therapeutic potential of interleukin-10. J Exp Med 217(1):e20190418.

Schoeler M and Caesar R, 2019. Dietary lipids, gut microbiota and lipid metabolism. Rev Endocr Metab Disord 20:461–472.

Shen C-L, Wang R, Santos JM, *et al*., 2024. Ginger alleviates mechanical hypersensitivity and anxio-depressive behavior in rats with diabetic neuropathy through beneficial actions on gut microbiome composition, mitochondria, and neuroimmune cells of colon and spinal cord. Nutr Res N Y N 124:73–84.

Visuthranukul C, Sriswasdi S, Tepaamorndech S, *et al*., 2024. Enhancing gut microbiota and microbial function with inulin supplementation in children with obesity. Int J Obes 48:1696–1704.

Wang Y, Xiang L, Wang Z, *et al*., 2020a. New anti-neuroinflammatory steroids against LPS induced NO production in BV2 microglia cells by microbial transformation of isorhodeasapogenin. Bioorganic Chem 101:103870.

Wang Y, Che M, Xin J, *et al*., 2020b. The role of IL-1β and TNF-α in intervertebral disc degeneration. Biomed Pharmacother Biomedecine Pharmacother 131:110660.

Wang Z, Xu J, Wang Y, *et al*., 2021. Total saponins from *Tupistra chinensis* baker inhibits growth of human gastric cancer cells in vitro and in vivo. J Ethnopharmacol 278:114323.

Wiertsema SP, van Bergenhenegouwen J, Garssen J, *et al*., 2021. The interplay between the gut microbiome and the immune system in the context of infectious diseases throughout life and the role of nutrition in optimizing treatment strategies. Nutrients 13(3):886.

Wong JT, Lane JK, Allan FK, *et al*., 2022. Reducing calf mortality in Ethiopia. Animals 12(16): 2126.

Xu J, Wang Z, Huang Y, *et al*., 2020. A spirostanol saponin isolated from *Tupistra chinensis* Baker simultaneously induces apoptosis and autophagy by regulating the JNK pathway in human gastric cancer cells. Steroids 164:108737.

Yang N, Xu J, Wang X, *et al*., 2022. The spatial landscape of the bacterial community and bile acids in the digestive tract of patients with bile reflux. Front Microbiol 13:835310.

Yi L, Zhu J, Li Q, *et al*., 2024. Panax notoginseng stems and leaves affect microbial community and function in cecum of duzang pigs. Transl Anim Sci 8: txad142.

Yo S, Matsumoto H, Gu T, *et al*., 2024. Exercise affects mucosa-associated microbiota and colonic tumor formation induced by Azoxymethane in high-fat-diet-induced obese mice. Microorganisms 12(5):957.

Yu J, Xiao X, Chen B, *et al*., 2024a. Synergistic and antagonistic activity of selected dietary phytochemicals against oxidative stress-induced injury in Cardiac H9c2 cells via the Nrf2 signaling pathway. Foods 13(15):2440.

Yu X, Ou J, Wang L, *et al*., 2024b. Gut microbiota modulate CD8(+) T cell immunity in gastric cancer through Butyrate/GPR109A/HOPX. Gut Microbes 16:2307542.

Zhang H, Yuan X, He Y, *et al*., 2024. A novel multiepitope fusion antigen as a vaccine candidate for the prevention of Enterotoxigenic *E. coli*-induced calf diarrhea. Vaccines 12(5):457.

Zhao L, Zhang H, Li N, *et al*., 2023. Network pharmacology, a promising approach to reveal the pharmacology mechanism of Chinese medicine formula. J Ethnopharmacol 309:116306.

Zhou B, Yuan Y, Zhang S, *et al*., 2020. Intestinal flora and disease mutually shape the regional immune system in the intestinal tract. Front Immunol 11:575.

Zhou Q, Qureshi N, Xue B, *et al*., 2022. Preventive and therapeutic effect of *Lactobacillus paracasei* ZFM54 on *Helicobacter pylori*-induced gastritis by ameliorating inflammation and restoring gastric microbiota in mice model. Front Nutr 9:972569.